Application of gain scheduled H∞ robust controllers to a magnetic bearing

Application of Gain Scheduled H_∞ Robust Controllers to a Magnetic Bearing

Fumio Matsumura, *Member, IEEE,* Toru Namerikawa, *Member, IEEE,*
Kazuhiko Hagiwara, and Masayuki Fujita, *Member, IEEE*

***Abstract*—This paper deals with the problem of an unbalance vibration zof the magnetic bearing system. We design a control system achieving the elimination of the unbalance vibration, using a loop shaping design procedure (LSDP). After the introduction of our experimental setup, a mathematical model of the magnetic bearing is shown. Then, the gain scheduled H_∞ robust controllers with free parameters are designed, based on the LSDP, so as to asymptotically reject the disturbances caused by unbalance on the rotor, even if the rotational speed of the rotor varies. Finally, several simulation results and experimental results show the effectiveness of this proposed methodology.**

I. Introduction

THIS PAPER proposes a gain scheduled robust control scheme for a rotating active magnetic bearing (AMB) system. By using magnetic bearings, a rotor is supported without any contact. The technique of contactless support for rotors has become very important in a variety of industrial applications.

Imbalance in the rotor mass causes vibration in rotating machines. Balancing of the rotor is very difficult—there is often a residual imbalance. However, this imbalance problem can be conquered by active control. It is well known that there are two methods for solving the above imbalance problem of magnetic bearings. The first method is to compensate for the unbalance forces by generating electro-magnetic forces that cancel these forces. The other method is to make the rotor rotate around its axis of inertia (automatic balancing). In this case no unbalance forces will be produced. There are several effective methods in the literature to achieve automatic balancing in the magnetic bearings [1]–[7]. If the magnetic bearings should be applied to precision machines, however, the rotor would be expected to rotate around its geometrical axis, hence the approach taken here is the first method.

This paper is a continuation of the previous research [8], [9] where we have considered both the problems of the coupling caused by gyroscopic effect and the problem of the vibration caused by unbalance on the rotor. In [9], the control system has been designed by using the loop shaping design procedure (LSDP) [10], and we have experimentally demonstrated its attenuating effect on the unbalance vibration.

Manuscript received October 2, 1995; revised March 19, 1996.

F. Matsumura, T. Namerikawa, and K. Hagiwara are with the Department of Electrical and Computer Engineering, Kanazawa University, 2-40-20 Kodatsuno, Kanazawa 920, Japan.

M. Fujita is with the School of Information Science, Japan Advanced Institute of Science and Technology, Hokuriku 15 Tatsunokuchi, Ishikawa 923-12, Japan.

Publisher Item Identifier S 1063-6536(96)06882-0.

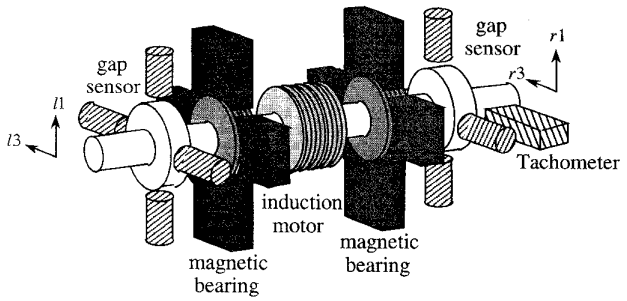

Fig. 1. Diagram of experimental machine.

The attenuation was only achieved at a fixed rotor operating speed in [8]. In this paper, we consider the elimination of the variable unbalance vibration caused by variable rotational speed. The vibrations caused by unbalance of the rigid rotor can be modeled as frequency-varying sinusoidal disturbances. Hence, in this paper, we propose the gain scheduled H_∞ controllers with the free parameter as a function of rotational speed to eliminate frequency-varying sinusoidal disturbances. This gain-scheduling approach is very simple and utilizes the free parameter of the H_∞ controller [11], [12]. The other gain-scheduling approaches for H_∞ control are reported in [13]–[16].

The outline of this paper is as follows. First, we introduce the magnetic bearing system and derive the mathematical model of the system [8], [17]. Next, we adopt the H_∞ problem with boundary constraints to the normalized left coprime factor robust stabilization H_∞ problem [12]; the conditions for existence of controller are derived with LSDP. Third, we design the controllers that achieve asymptotic disturbance rejection and robust stability. Finally, we present simulation and experimental results with the obtained H_∞ controllers, and indicate the effectiveness of this proposed approach.

II. Modeling

A. Magnetic Bearing System

The magnetic bearing system employed in this research is a four-axis controlled horizontal shaft magnetic bearing with symmetric structure. The axial motion is not controlled actively. The diagram of the experimental machine is shown in Fig. 1. The diameter of the rotor is 96 mm and its span is 660 mm. A three-phase induction motor (1 kW, four poles) is located at the center of the rotor. Around the rotor, four pairs of electromagnets are arranged radially, and four pairs of eddy-current type gap sensors are located on outside of

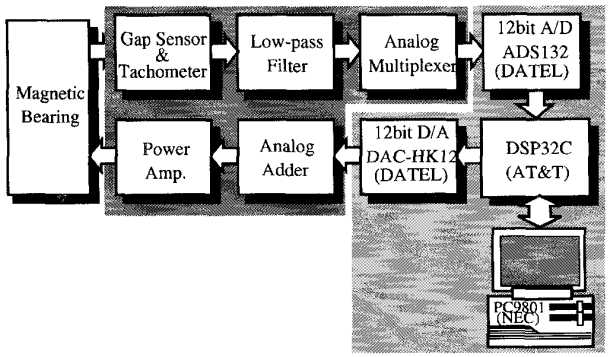

Fig. 2. Digital control system.

the electromagnets. Further, this system employs a tachometer in order to measure the rotational speed of the rotor. The experimental machine is controlled by a digital control system that consists of a 32-b floating point digital signal processor (DSP) DSP32C (AT&T), 12-b A/D converters, and 12-b D/A converters. Using these components, the final discrete-time controllers including a free parameter are computed on the DSP. The diagram of digital control system is shown in Fig. 2.

B. Mathematical Model of the Magnetic Bearing

In this section, we derive the state equation of a magnetic bearing system with the following assumptions:

1) The rotor is rigid and has no unbalance.
2) All electromagnets are identical.
3) Attractive force of an electromagnet is in proportion to (electric current/gap length)^2.
4) The resistance and the inductance of the electromagnet coil are constant and independent of the gap length.
5) Small deviations from the equilibrium point are treated.

Based on the above assumptions, a mathematical model of a magnetic bearing has been derived in [17], and the obtained result is as follows:

$$\begin{bmatrix}\dot{x}_v\\ \dot{x}_h\end{bmatrix} = \begin{bmatrix}A_v & pA_{vh}\\ -pA_{vh} & A_h\end{bmatrix}\begin{bmatrix}x_v\\ x_h\end{bmatrix} + \begin{bmatrix}B_v & 0\\ 0 & B_h\end{bmatrix}\begin{bmatrix}u_v\\ u_h\end{bmatrix} + p^2\begin{bmatrix}E_v\\ E_h\end{bmatrix}w \tag{1}$$

$$\begin{bmatrix}y_v\\ y_h\end{bmatrix} = \begin{bmatrix}C_v & 0\\ 0 & C_h\end{bmatrix}\begin{bmatrix}x_v\\ x_h\end{bmatrix} \tag{2}$$

where the subscripts v and h in the vectors and the matrices stand for the vertical motion and the horizontal motion of the magnetic bearing, respectively. In addition, the subscript vh stands for the coupling term between the vertical motion and the horizontal motion, and p denotes the rotational speed of the rotor. Each vector in (1) and (2) can be defined as

$$\begin{aligned} x_v &= [g_{l1} \quad g_{r1} \quad \dot{g}_{l1} \quad \dot{g}_{r1} \quad i_{l1} \quad i_{r1}]^T\\ x_h &= [g_{l3} \quad g_{r3} \quad \dot{g}_{l3} \quad \dot{g}_{r3} \quad i_{l3} \quad i_{r3}]^T\\ u_v &= [e_{l1} \quad e_{r1}]^T, \quad u_h = [e_{l3} \quad e_{r3}]^T\\ w &= \begin{bmatrix}\epsilon\sin(pt+\kappa)\\ \tau\cos(pt+\lambda)\\ \epsilon\cos(pt+\kappa)\\ \tau\sin(pt+\lambda)\end{bmatrix} \end{aligned} \tag{3}$$

where

g_j	deviations from the steady gap lengths between the electromagnets and the rotor;
i_j	deviations from the steady currents of the electromagnets;
e_j	deviations from the steady voltages of the electromagnets;
$\epsilon, \tau, \kappa, \lambda$	unbalance parameters [5], [17];
$(j = l1, r1, l3, r3)$.	

The subscripts l and r denote the left- and right-hand sides of the rotor, respectively, and the subscripts "1" and "3" denote one of the vertical directions and one of the horizontal directions of the rotor, respectively. Each matrix in (1) and (2) can be defined as follows:

$$A_v := \begin{bmatrix}0 & I & 0\\ A_1 + A_2A_{4v} & 0 & A_2A_{5v}\\ 0 & 0 & -(R/L)I\end{bmatrix}$$

$$A_h := \begin{bmatrix}0 & I & 0\\ A_1 + A_2A_{4h} & 0 & A_2A_{5h}\\ 0 & 0 & -(R/L)I\end{bmatrix}$$

$$A_{vh} := \begin{bmatrix}0 & 0 & 0\\ 0 & A_3 & 0\\ 0 & 0 & 0\end{bmatrix}, \quad B_v = B_h := \begin{bmatrix}0\\ 0\\ (1/L)I\end{bmatrix}$$

$$C_v = C_h := [I \quad 0 \quad 0]$$

$$E_v := \begin{bmatrix}0\\ E_{1v}\\ 0\end{bmatrix}, \quad E_h := \begin{bmatrix}0\\ E_{1h}\\ 0\end{bmatrix}$$

$$A_1 := \frac{\alpha}{l_l + l_r} \cdot \begin{bmatrix}(l_r - l_m)\left(\frac{1}{m} - \frac{l_l l_m}{J_y}\right) & (l_l - l_m)\left(\frac{1}{m} - \frac{l_l l_m}{J_y}\right)\\ (l_r - l_m)\left(\frac{1}{m} + \frac{l_r l_m}{J_y}\right) & (l_l - l_m)\left(\frac{1}{m} + \frac{l_r l_m}{J_y}\right)\end{bmatrix}$$

$$A_2 := \begin{bmatrix}-\frac{1}{m} - \frac{l_l^2}{J_y} & -\frac{1}{m} + \frac{l_l l_r}{J_y}\\ -\frac{1}{m} + \frac{l_l l_r}{J_y} & -\frac{1}{m} - \frac{l_r^2}{J_y}\end{bmatrix}$$

$$A_3 := \frac{J_x}{J_y(l_l + l_r)}\begin{bmatrix}-l_l & l_l\\ l_r & -l_r\end{bmatrix}$$

$$A_{4v} := -\frac{2}{W}\mathrm{diag}[F_{l1} + F_{l2}, F_{r1} + F_{r2}]$$

$$A_{4h} := -\frac{2}{W}\mathrm{diag}[F_{l3} + F_{l4}, F_{r3} + F_{r4}]$$

$$A_{5v} := 2\mathrm{diag}\left[\frac{F_{l1}}{I_{l1}} + \frac{F_{l2}}{I_{l2}}, \frac{F_{r1}}{I_{r1}} + \frac{F_{r2}}{I_{r2}}\right]$$

$$A_{5h} := 2\mathrm{diag}\left[\frac{F_{l3}}{I_{l3}} + \frac{F_{l4}}{I_{l4}}, \frac{F_{r3}}{I_{r3}} + \frac{F_{r4}}{I_{r4}}\right]$$

$$E_{1v} := \begin{bmatrix}-1 & l_l\left(1 - \frac{J_x}{J_y}\right) & 0 & 0\\ -1 & -l_r\left(1 - \frac{J_x}{J_y}\right) & 0 & 0\end{bmatrix}$$

$$E_{1h} := \begin{bmatrix}0 & 0 & 1 & l_l\left(1 - \frac{J_x}{J_y}\right)\\ 0 & 0 & 1 & -l_r\left(1 - \frac{J_x}{J_y}\right)\end{bmatrix}.$$

TABLE I
PARAMETERS OF EXPERIMENTAL MACHINE

Parameter	Symbol	Value	Unit
Mass of the Rotor	m	1.39×10^{1}	kg
Moment of Inertia about X	J_x	1.348×10^{-2}	kg · m^2
Moment of Inertia about Y	J_y	2.326×10^{-1}	kg · m^2
Distance between Center of Mass and Left Electromagnet	l_l	1.30×10^{-1}	m
Distance between Center of Mass and Right Electromagnet	l_r	1.30×10^{-1}	m
Distance between Center of Mass and Motor	l_m	0	m
Steady Attractive Force	$F_{l1,r1}$	9.09×10	N
	$F_{l2\sim l4}$	2.20×10	N
	$F_{r2\sim r4}$	2.20×10	N
Steady Current	$I_{l1,r1}$	6.3×10^{-1}	A
	$I_{l2\sim l4}$	3.1×10^{-1}	A
	$I_{r2\sim r4}$	3.1×10^{-1}	A
Steady Gap	W	5.5×10^{-4}	m
Resistance	R	1.07×10	Ω
Inductance	L	2.85×10^{-1}	H

For the notations, as well as the parameter values, see Table I. In the above equations, α denotes the coefficient of the force which occurs when the rotor eccentrically deviates, and hence we set $\alpha = 0$. The numerical values of these matrices can easily be obtained with Table I, and the results are in [8].

III. H_∞ GAIN SCHEDULING

In order to attenuate the unbalance vibration of the rotor, we design the robust H_∞ controllers which asymptotically achieve the sinusoidal disturbance rejection. As is well known, the controllers must have the imaginary poles at the frequencies corresponding to the rotational speed to possess high stiffness. For such a control system design, the LSDP based on the normalized left coprime factor (LCF) robust stabilization method [10] is employed. Using the free parameter method which has been proposed in [9], it is possible to obtain the gain scheduled controllers by the free parameter as the function of rotational speed. We therefore show the condition for the existence of controllers, by adopting the control problem with boundary constraints [11] to the normalized LCF robust stabilization problem, and we design a robust controller which satisfies the derived specifications using the LSDP.

Let (N, M) represent a normalized left coprime factorization of a plant G. Let these coprime factors be assumed to have uncertainties Δ_N, Δ_M and let G_Δ represent the plant with these uncertainties

$$\begin{aligned} G_\Delta &= M_\Delta^{-1} N_\Delta \\ &= (M + \Delta_M)^{-1}(N + \Delta_N) \end{aligned} \tag{4}$$

where N_Δ and M_Δ represent a left coprime factorization of G_Δ, and

$$\Delta = \{[\Delta_N, \quad \Delta_M] \in RH_\infty; \|[\Delta_N, \quad \Delta_M]\|_\infty < \varepsilon\}. \tag{5}$$

G_Δ can be written in the form of an upper linear fractional transformation (ULFT) as follows:

$$\begin{aligned} G_\Delta &= F_U(P, \Delta) \\ &= P_{22} + P_{21}\Delta(I - P_{11}\Delta)^{-1}P_{12} \end{aligned} \tag{6}$$

where

$$P = \left[\begin{array}{c|c} P_{11} & P_{12} \\ \hline P_{21} & P_{22} \end{array}\right] = \left[\begin{array}{c|c} 0 & I \\ \hline M^{-1} & G \\ \hline M^{-1} & G \end{array}\right]. \tag{7}$$

The robust stabilization problem for the *perturbed* plant G_Δ can be treated as the next H_∞ control problem

$$\left\| \begin{bmatrix} K \\ I \end{bmatrix} (I - GK)^{-1} M^{-1} \right\|_\infty \leq \varepsilon^{-1} := \gamma. \tag{8}$$

It is known that the solution of this problem and the largest number of ϵ $(= \epsilon_{\max} := \gamma_{\min}^{-1})$ can be obtained by solving two Riccati equations without iterative procedure. All controllers K satisfying (8) are given by

$$K = F_L(K_a, \Phi) := K_{11} + K_{12}\Phi(I - K_{22}\Phi)^{-1}K_{21} \tag{9}$$

where

$$K_a = \left[\begin{array}{c|c} K_{11} & K_{12} \\ \hline K_{21} & K_{22} \end{array}\right] \tag{10}$$

$$\|\Phi\|_\infty \leq 1. \tag{11}$$

For the calculation of K_a and $\epsilon_{\max}$, see [10]. In order to eliminate the unbalance vibration of the rotor, which can be modeled as sinusoidal disturbances [18], the robust controller should be designed to asymptotically achieve sinusoidal disturbance rejection. In this case, as is well known, the controller must have the imaginary poles at the frequencies corresponding to the rotational speed of the rotor [11], [12].

Hence, for the achievement of sinusoidal disturbance rejection whose frequency is ω_0 [rad/s], $K(s)$ is required to satisfy

$$K(\pm j\omega_0) = \infty \Leftrightarrow \{I - G(\pm j\omega_0)K(\pm j\omega_0)\}^{-1} = 0. \quad (12)$$

We then derive the conditions, by adopting the H_∞ problem with boundary constraints [12] shown in the Appendix, to this problem whereby there exist the controllers satisfying both (8) and (12). The boundary constraint $\{L, \Pi, \Psi\}$ corresponding to (12) is given by

$$L = [0 \quad I], \quad \Pi = M(\pm j\omega_0), \quad \Psi = 0. \quad (13)$$

The basic constraint $\{L_B, \Psi_B\}$ in (36) (in the Appendix) is described by

$$L_B = P_{12}^{\perp}(\pm j\omega_0) = [-G(\pm j\omega_0) \quad I] \quad (14)$$

$$\Psi_B = P_{12}^{\perp}(\pm j\omega_0)P_{11}(\pm j\omega_0) = M^{-1}(\pm j\omega_0). \quad (15)$$

It is obvious that $\{L, \Pi, \Psi\}$ is satisfying condition (b) in Theorem A, and the extended boundary constraint $\{\hat{L}, \hat{\Psi}\}$ in (37) (in the Appendix) is given by

$$\hat{L} = \begin{bmatrix} -G(\pm j\omega_0) & I \\ 0 & I \end{bmatrix}, \quad \hat{\Psi} = \begin{bmatrix} I \\ 0 \end{bmatrix}. \quad (16)$$

After some straightforward calculation, we have

$$\gamma\overline{\sigma}(N(\pm j\omega_0)) > 1 \quad (17)$$

where

$$\overline{\sigma}(N(\pm j\omega_0)) = \left(\frac{\overline{\sigma}^2(G(\pm j\omega_0))}{1 + \overline{\sigma}^2(G(\pm j\omega_0))}\right)^{1/2}$$

$\overline{\sigma}(\bullet)$: the maximum singular value

from condition c) of Theorem A.

If we choose free parameter $\Phi(s)$ such that

$$\Phi(\pm j\omega_0) = K_{22}^{-1}(\pm j\omega_0) \quad (18)$$

under the conditions (11) and (17), it can be seen that we obtain the controller with the imaginary poles at $\pm j\omega_0$ from (9). Based on this, we design the control system using the LSDP [10]. The procedure is briefly outlined below.

Loop Shaping Design Procedure (LSDP):

Step 1—Loop Shaping: Selecting shaping function W_1 and W_2, the singular values of the nominal plant G are shaped to have a desired open-loop shape. Let G_S represent this shaped plant

$$G_S = W_2GW_1. \quad (19)$$

W_1 and W_2 should be selected such that G_S has no hidden unstable modes.

Step 2—Robust Stabilization: The maximum stability margin $\epsilon_{\max}$ is calculated. If $\epsilon_{\max} \ll 1$, return to Step 1, then W_1 and W_2 should be selected again. Otherwise, γ is appropriately selected as $\gamma \geq \gamma_{\min} = \epsilon_{\max}^{-1}$ and K_a is calculated. The free parameter Φ is selected as in (18) under these conditions, then the H_∞ controller $K_\infty(s)$ is synthesized for G_S from (9).

Step 3—Final Controller: The final controller K can be obtained by the combination of W_1, W_2, and K_∞

$$K = W_1K_\infty W_2. \quad (20)$$

In this procedure, $\epsilon_{\max}$ is treated as a design indicator rather than the maximum stability margin of G_S. Thus, we can design the robust controllers achieving sinusoidal disturbance rejection asymptotically using the LSDP. Moreover, utilizing the free parameter for such design, it is possible to obtain the gain scheduled controllers, by scheduling the free parameter as the function of rotational speed of the rotor, which achieve the elimination of the unbalance vibration even if the rotational speed of the rotor varies.

The H_∞ controller $K_\infty(s)$ with the free parameter Φ is shown as follows:

$$K_\infty = F_L(K_a, \Phi) \quad (21)$$

where

$$K_a = \left[\begin{array}{c|cc} A_{K_a} & B_{K_a1} & B_{K_a2} \\ \hline C_{K_a1} & D_{K_a11} & D_{K_a12} \\ C_{K_a2} & D_{K_a21} & D_{K_a22} \end{array}\right], \quad \Phi = \left[\begin{array}{c|c} A_\Phi & C_\Phi \\ \hline B_\Phi & D_\Phi \end{array}\right].$$

Hence (22), as shown at the bottom of the page, where

$$X_0 = (I - D_\Phi D_{K_a22})^{-1}C_\Phi, \quad Y_0 = B_\Phi(I - D_{K_a22}D_\Phi)^{-1}$$
$$Z_0 = (I - D_\Phi D_{K_a22})^{-1}D_\Phi.$$

Therefore the final H_∞ controller K is as

$$K = W_1K_\infty W_2$$

where we define the weighting functions W_1 and W_2 as

$$W_1 = \left[\begin{array}{c|c} A_{W1} & C_{W1} \\ \hline B_{W1} & D_{W1} \end{array}\right]$$

W_2: diagonal constant matrix (23)

then (24), as shown at the bottom of the next page. The block diagram of this final controller is shown in Fig. 3.

$$K_\infty := \left[\begin{array}{cc|c} A_{K_\infty11} & A_{K_\infty12} & B_{K_\infty1} \\ A_{K_\infty21} & A_{K_\infty22} & B_{K_\infty2} \\ \hline C_{K_\infty1} & C_{K_\infty2} & D_{K_\infty} \end{array}\right]$$
$$= \left[\begin{array}{cc|c} A_{K_a} + B_{K_a2}Z_0C_{K_a2} & B_{K_a2}X_0 & B_{K_a1} + B_{K_a2}Z_0D_{K_a21} \\ Y_0C_{K_a2} & A_\Phi + Y_0D_{K_a22}C_\Phi & Y_0D_{K_a21} \\ \hline C_{K_a1} + D_{K_a12}Z_0C_{K_a2} & D_{K_a12}X_0 & D_{K_a11} + D_{K_a12}Z_0D_{K_a21} \end{array}\right] \quad (22)$$

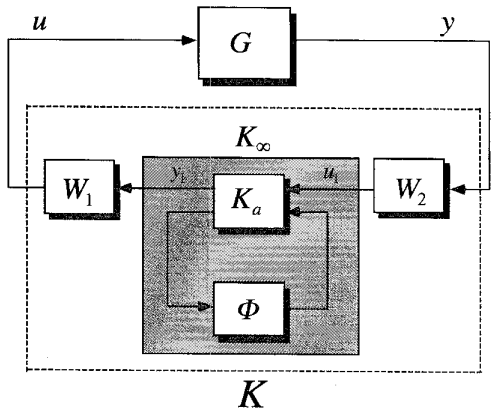

Fig. 3. The gain scheduled H_∞ controller with the free parameter Φ.

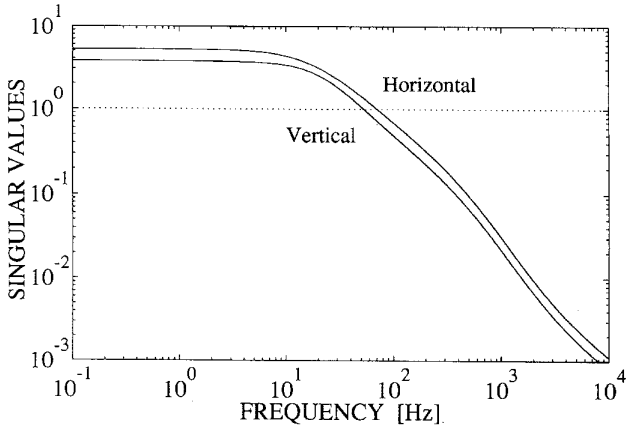

Fig. 4. Magnitude of $\gamma\sigma(N_S)$.

IV. Controller Design

In this section, the feedback controllers are designed with the LSDP. We assume rotational speed $p = 0$ in the nominal plant G. In this case, we can see that there is no coupling between the vertical motion and horizontal motion in (1). Therefore, the plant model can be separated into the vertical plant $G_v(s) := C_v(sI - A_v)^{-1}B_v$ and the horizontal plant $G_h(s) := C_h(sI - A_h)^{-1}B_h$, respectively

$$G = \begin{bmatrix} G_v & 0 \\ 0 & G_h \end{bmatrix}. \tag{25}$$

Then, two controllers will be designed for each plant, respectively. The final controller K for the entire plant G will be constructed with a combination of these controllers

$$K = \begin{bmatrix} K_v & 0 \\ 0 & K_h \end{bmatrix} \tag{26}$$

where K_v denotes the controller for the vertical plant and K_h denotes the controller for the horizontal plant. The shaping functions and the design parameters are selected as follows:

(v) *Design for vertical motion*:

$$W_{1v}(s) = \frac{1300(1 + s/(2\pi \cdot 5))(1 + s/(2\pi \cdot 35))(1 + s/(2\pi \cdot 50))}{(1 + s/(2\pi \cdot 0.01))(1 + s/(2\pi \cdot 700))(1 + s/(2\pi \cdot 1200))} \cdot \begin{bmatrix} 1 & 0 \\ 0 & 1 \end{bmatrix} \tag{27}$$

$$W_{2h}(s) = 10000 \begin{bmatrix} 1 & 0 \\ 0 & 1 \end{bmatrix} \tag{28}$$

$$\epsilon_{v\_\max} = 0.199\,44, \quad \epsilon_v^{-1} = \gamma_v = 5.25. \tag{29}$$

(h) *Design for horizontal motion:*

$$W_{1h}(s) = \frac{1100(1 + s/(2\pi \cdot 5))(1 + s/(2\pi \cdot 25))(1 + s/(2\pi \cdot 40))}{(1 + s/(2\pi \cdot 0.01))(1 + s/(2\pi \cdot 700))(1 + s/(2\pi \cdot 1200))} \cdot \begin{bmatrix} 1 & 0 \\ 0 & 1 \end{bmatrix} \tag{30}$$

$$W_{2h}(s) = 10000 \begin{bmatrix} 1 & 0 \\ 0 & 1 \end{bmatrix} \tag{31}$$

$$\epsilon_{h\_\max} = 0.274\,32, \quad \epsilon_h^{-1} = \gamma_h = 3.75. \tag{32}$$

In this design, verifying the condition (17), it can be seen from Fig. 4 that it is possible to design the controllers below $\omega_0 = 324.63$ [rad/s] ($p = 3100$ [r/min]). Hence we design the controllers within the above bound. In order to satisfy the condition (11), the free parameters are selected as

$$\Phi_d(s) = C_{\Phi d}(sI - A_{\Phi d})^{-1}B_{\Phi d} \tag{33}$$

$$K = \left[\begin{array}{ccc|c} A_{W1} & B_{W1}C_{K_\infty 1} & B_{W1}C_{K_\infty 2} & B_{W1}D_{K_\infty}W_2 \\ 0 & A_{K_\infty 11} & A_{K_\infty 12} & B_{K_\infty 1}W_2 \\ 0 & A_{K_\infty 21} & A_{K_\infty 22} & B_{K_\infty 2}W_2 \\ \hline C_{W1} & D_{W1}C_{K_\infty 1} & D_{W1}C_{K_\infty 2} & D_{W1}D_{K_\infty}W_2 \end{array}\right]$$
$$= \left[\begin{array}{ccc|c} A_{W1} & B_{W1}(C_{K_a 1} + D_{K_a 12}Z_0C_{K_a 2}) & B_{W1}D_{K_a 12}X_0 & B_{W1}(D_{K_a 11} + D_{K_a 21}Z_0D_{K_a 21})W_2 \\ 0 & A_{K_a} + B_{K_a 2}Z_0C_{K_a 2} & B_{K_a 2}X_0 & (B_{K_a 1} + B_{K_a 2}Z_0D_{K_a 21})W_2 \\ 0 & Y_0C_{K_a 2} & A_\Phi + Y_0D_{K_a 22}C_\Phi & Y_0D_{K_a 21}W_2 \\ \hline C_{W1} & D_{W1}(C_{K_a 1} + D_{K_a 12}Z_0C_{K_a 2}) & D_{W1}D_{K_a 12}X_0 & D_{W1}(D_{K_a 11} + D_{K_a 12}Z_0D_{K_a 21})W_2 \end{array}\right] \tag{24}$$

TABLE II
PARAMETERS a_d, b_d OF FREE PARAMETERS

Rotational speed (rpm)	a_v	b_v	a_h	b_h
$1000 \sim 1600$	2800	8	2800	8
$1600 \sim 2200$		16		16
$2200 \sim 2600$	2500	25	2500	27
$2600 \sim 2900$		37		36
$2900 \sim 3100$				40

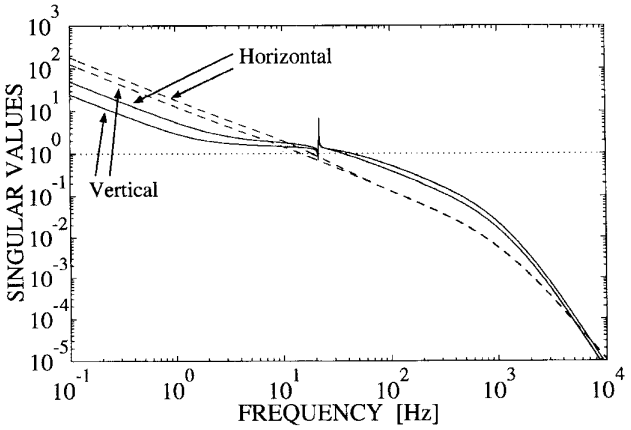

Fig. 5. Open-loop transfer functions GK [—] and the shaped plant G_S [- -].

where

$$A_{\Phi d} = \begin{bmatrix} -a_d & 0 \\ 0 & -b_d \end{bmatrix}, \quad B_{\Phi d} = \begin{bmatrix} I \\ I \end{bmatrix}$$

$$C_{\Phi d} = [C_{\Phi 1 d} \quad C_{\Phi 2 d}]$$

$$C_{\Phi 1 d} = \frac{(a_d^2 + \omega_0^2)}{\omega_0 (a_d - b_d)} \cdot \{\omega_0 \Re(K_{22d}^{-1}(j\omega_0)) + b_d \Im(K_{22d}^{-1}(j\omega_0))\}$$

$$C_{\Phi 2 d} = \frac{(b_d^2 + \omega_0^2)}{\omega_0 (b_d - a_d)} \cdot \{\omega_0 \Re(K_{22d}^{-1}(j\omega_0)) + a_d \Im(K_{22d}^{-1}(j\omega_0))\}$$

$$(d = v, r).$$

Furthermore, in order to satisfy the condition (11), the parameters a_d and b_d of $A_{\Phi d}$ and $C_{\Phi d}$ are, respectively, adjusted as shown in Table II. When we obtain the shaped plants, a model reduction technique has been employed. The procedure of the model reduction is the nominal plant model reduction procedure as shown in [10, Procedure 5.5]. The order of each of the shaped plants has been reduced from 12 states to 8. As a consequence, the final controller has 36 states. As an example, we show the frequency response of the designed controller, which is denoted by K_{1300}, with $\omega_0 = 136.14$ [rad/s]($p = 1300$ [r/min]). The singular values of the shaped plants and the open loop transfer functions are shown in Fig. 5, and Fig. 6 shows the singular values of the sensitivity functions. From these figures, we can see that sensitivity approaches zero at the frequency ω_0.

In this design, we ignored the interference terms, which express the gyroscopic effect, as $p = 0$. We therefore verify the robust stability of this system against changes in the rotational

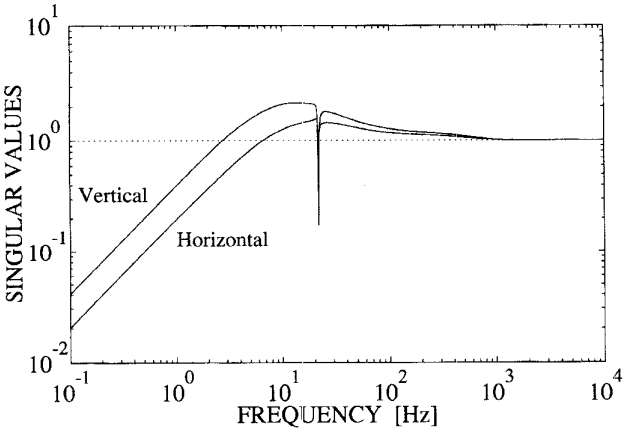

Fig. 6. $\sigma((I - GK)^{-1})$.

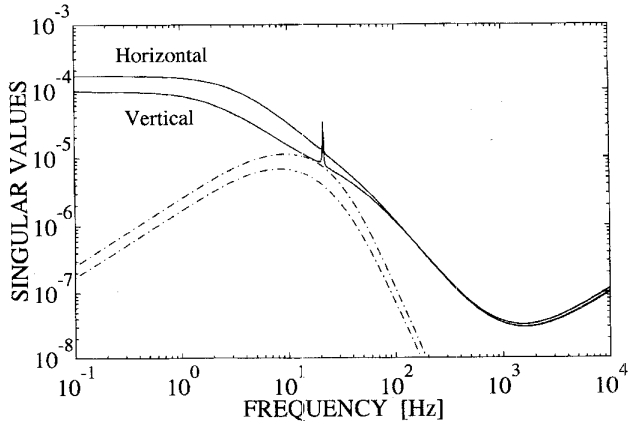

Fig. 7. $1/\sigma(K(I - GK)^{-1})$ [—] and $\sigma(\Delta_p)$ [- · -].

speed of the rotor. Let the perturbed plant ($p \neq 0$) be denoted by G_p and the additive perturbation Δ_p from G is as follows:

$$\Delta_p = G_p - G. \tag{34}$$

Then the robust stability is guaranteed within the the following inequality:

$$\overline{\sigma}(\Delta_p) < \frac{1}{\overline{\sigma}(K(I - GK)^{-1})}. \tag{35}$$

In Fig. 7, the singular values $1/\sigma(K(I - GK)^{-1})$ and $\sigma(\Delta_p)$ at $\omega_0 = 1675.5$ [rad/s] ($p = 16\,000$ [r/min]) are plotted. From this analysis, we can see the closed-loop system is stable at $\omega_0 \leq 1675.5$ [rad/s].

V. SIMULATION RESULTS

The simulation results based on the derived nominal mathematical model, which are carried out by using SIMULINK [19], are shown in Figs. 8 and 9. These figures show the displacement on the left side of the rotor when the rotational speed is varied at the rate of 2 r/min/s.

For the comparison, the linear time invariant H_∞ controller K_{1300} was employed, where the controller K_{1300} has the fixed

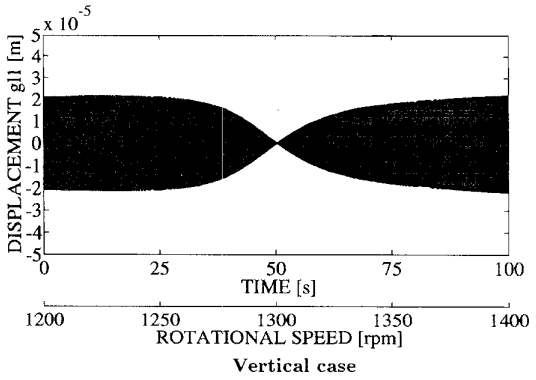

(a)

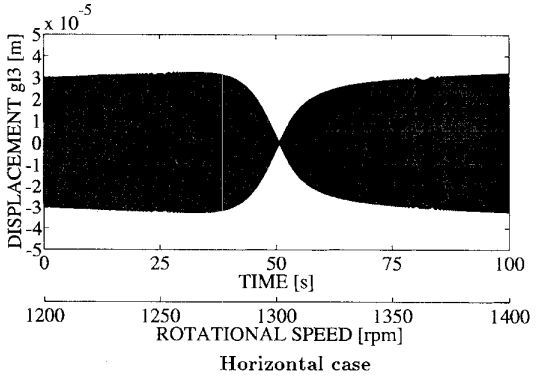

(b)

Fig. 8. Displacement versus rotational speed with the controller K_{1300}. (a) Vertical case. (b) Horizontal case.

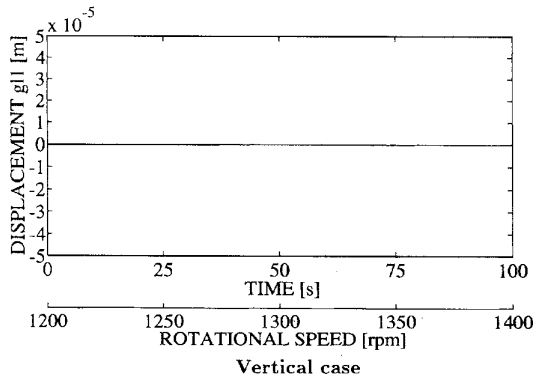

(a)

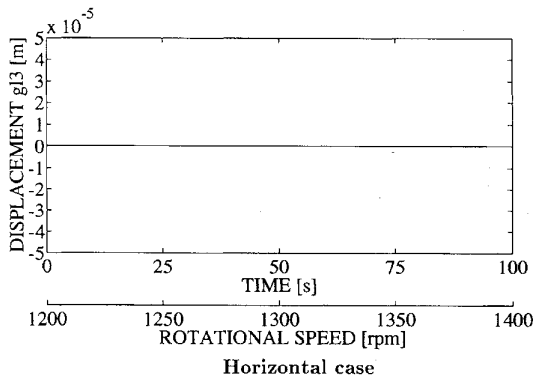

(b)

Fig. 9. Displacement versus rotational speed with the gain scheduled H_∞ controller. (a) Vertical case. (b) Horizontal case.

pole at $f_0 = 1300/60 = 21.7$ Hz and no gain-scheduling is adopted.

The results with the time-invariant H_∞ controller K_{1300} are shown in Fig. 8(a) and (b), which indicate the response of the rotor when the rotational speed is varied from 1200 to 1400 r/min. The corresponding results with the gain scheduled H_∞ controller K are shown in Fig. 9(a) and (b), respectively.

Figs. 8(a) and 9(a) show the vertical rotor displacement with the variable rotating speed, and Figs. 8(b) and 9(b) show the horizontal rotor displacement. From these simulation results, it can be seen that even if the rotational speed of the rotor varies, the unbalance vibration of the rotor is eliminated by the proposed gain scheduled H_∞ robust controllers.

VI. Experimental Results

We have carried out experiments using the experimental machine shown in Fig. 1. In order to evaluate the practical effect of this proposed approach, the experimental tests were run within the limits of the rotational speed from 1000 to 1600 r/min (see Table II).

The designed continuous-time controllers, K_{1300} and gain scheduled H_∞ controller are discretized via the well-known Tustin transform at the sampling rates of 252 and 415 μs, respectively.

The controller K_{1300} is a linear invariant dynamical controller, hence the computing burden for real-time calculation of control input is only matrix multiplication and addition.

On the other hand, for the implementation of the gain scheduled H_∞ controller $K(\Phi)$, we have to renew $K(\Phi)$ every sampling period by using (24). After this has been obtained, the control input u is calculated; it takes longer for the implementation of $K(\Phi)$.

All through the experiments, a small weight (20 g) is attached at the left side of the rotor in Fig. 1 to increase the residual unbalance.

We have measured the orbits of the center of the rotor for a period of 0.5 s under several conditions. Fig. 10(a)–(c) shows the results with K_{1300}, and Fig. 10(d)–(f) shows the results with gain scheduled H_∞ controller, at 1100, 1300, and 1500 r/min, respectively. Comparing the gain scheduled H_∞ controller K with K_{1300}, the results with gain scheduled H_∞ controller K indicate better performance than those with K_{1300} in the elimination of the unbalance vibration, except at 1300 r/min.

However, it is well known that direct switching and interpolation between the controllers does not capture the dynamic effects and may lead to instability, even if the controllers can stabilize the closed-loop system for each frozen value in

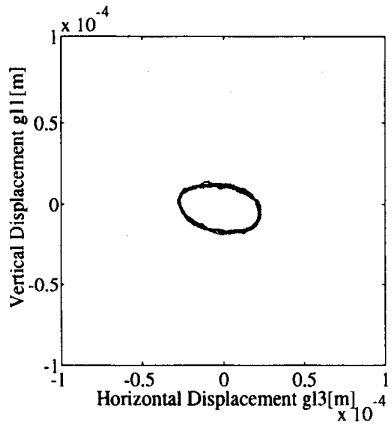

The fixed H_∞ controller K_{1300} rotational speed: 1100 [rpm]

(a)

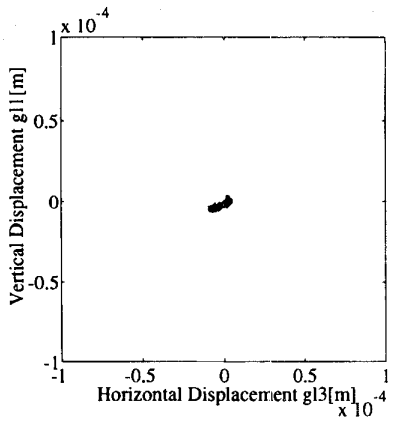

The fixed H_∞ controller K_{1300} rotational speed: 1300 [rpm]

(b)

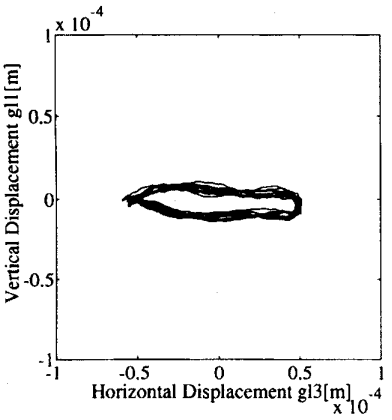

The fixed H_∞ controller K_{1300} rotational speed: 1500 [rpm]

(c)

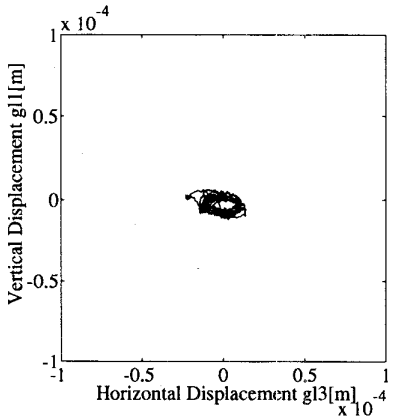

The gain scheduled H_∞ controller rotational speed: 1100 [rpm]

(d)

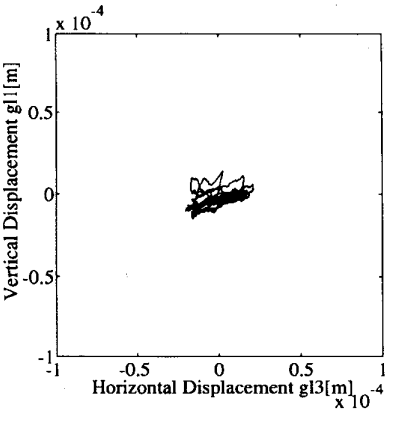

The gain scheduled H_∞ controller rotational speed: 1300 [rpm]

(e)

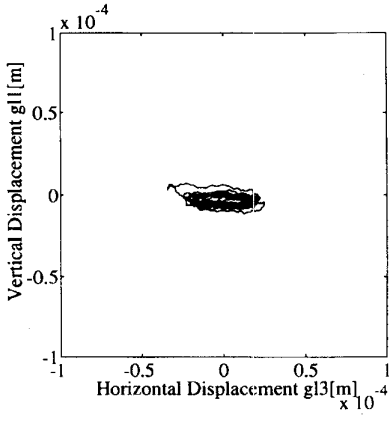

The gain scheduled H_∞ controller rotational speed: 1500 [rpm]

(f)

Fig. 10. Orbits of the center of the rotor.

the parameter space. This is especially true if the scheduled parameter changes rapidly.

By the numerical simulation, we have confirmed that the closed-loop system is stable when the rotational speed changes at the rate of 2 r/min/s or less (see Figs. 8 and 9). If the rotational speed changes more than 2 r/min/s, the system becomes unstable.

While the rotor speed should be able to vary, for many applications it does not need to vary quickly. For this rotor, limited power and the safety of the induction motor dictate that the rotational speed can not be changed rapidly.

From a theoretical point of view, gain scheduled H_∞ controller should completely attenuate the unbalance vibration even if the rotational speed of the rotor varies. However, this level of performance has not been achieved experimentally. This performance deterioration may be due to the measurement precision of the rotating speed. Gain scheduled H_∞ controller very strongly relies on the accuracy of the rotational speed. Since the notch in the sensitivity function is very narrow, error in the measurement of rotational speed may significantly deteriorate performance.

Further investigation and experiments examining the effects of rotational speed and the scheduled parameter's changing rate will be made in the future.

VII. Conclusion

In this paper, we proposed a gain scheduled H_∞ robust control scheme with free parameters for the elimination of unbalance vibration in a magnetic bearing supported rotor. We treated the changing unbalance vibration caused by varying rotational speed as a known frequency-varying disturbance, and adjusted the controller gain according to the rotational speed of the rotor using the free parameter Φ of the H_∞ controller. The obtained controller K has high gain at the operating frequency.

First, the dynamics of the AMB system was considered and a nominal mathematical model for the system was derived. Next, the conditions for the existence of controllers were derived, and we designed the gain scheduled H_∞ robust controllers using LSDP, which rejected the sinusoidal disturbance of the varying rotor speed.

Finally, simulations and experimental results showed the effectiveness of this proposed method.

Appendix

- *Definition A*: "H_∞ problem with boundary constraints." Find the $K(s)$ satisfying

$$\begin{array}{ll}(s1) & K(s) \text{ stabilizes } F_U(P,0)\\ (s2) & \|P_{zw}\|_\infty \le \varepsilon^{-1} := \gamma\\ (s3) & LP_{zw}(j\omega)\Pi = \Psi\end{array}$$

  where $P_{zw} = F_L(P,K)$.
- *Definition B*: "Basic constraints"

$$L_B := P_{12}^{\perp}(j\omega), \quad \Psi_B := P_{12}^{\perp}(j\omega)P_{11}(j\omega) \tag{36}$$

  where $P_{12}^{\perp}(s)P_{12}(s) = 0$.
- *Definition C*: "Extended constraints"

$$\hat{L} := \begin{bmatrix} L_B \\ L \end{bmatrix}, \quad \hat{\Psi} := \begin{bmatrix} \Psi_B\Pi \\ \Psi \end{bmatrix} \tag{37}$$

  where $\hat{L}$ and $\hat{\Psi}$ are row full rank.

Theorem A: H_∞ problem with boundary constraints $\{L, \Pi, \Psi\}$ is solvable, iff the following three conditions hold:

a) The H_∞ problem is solvable.
b) Rank $\begin{bmatrix} L_B & \Psi_B \\ L & \Pi \end{bmatrix}$ = rank $\begin{bmatrix} L_B \\ L \end{bmatrix}$.
c) $\hat{L}\hat{L}^* > \gamma^2\hat{\Psi}(\Pi^*\Pi)^{-1}\hat{\Psi}^*$.

Acknowledgment

The authors would like to extend their deepest gratitude to K. Hatake and M. Hirai for helpful discussions.

References

[1] B. Shafai, S. Beale, P. LaRocc, and E. Cusson, "Magnetic bearing control systems and adaptive forced balancing," *IEEE Contr. Syst. Mag.*, vol. 14, no. 2, pp. 4–13, Apr. 1994.
[2] T. Mizuno and T. Higuchi, "Compensation for unbalance in magnetic bearing systems," *Trans. SICE*, vol. 20, no. 12, pp. 23–29, Dec. 1984 (in Japanese).
[3] A. M. Mohamed and F. P. Emad, "Conical magnetic bearing with radial and thrust control," *IEEE Trans. Automat. Contr.*, vol. 37, no. 12, pp. 1859–1868, Dec. 1992.
[4] A. M. Mohamed and I. J. Busch-Vishniac, "Imbalance compensation and automation balancing in magnetic bearing systems using the Q-parameterization theory," *IEEE Trans. Contr. Syst. Technol.*, vol. 3, no. 2, pp. 202–211, June 1995.
[5] F. Matsumura, M. Fujita, and K. Okawa, "Modeling and control of magnetic bearing systems achieving a rotation around the axis of inertia," in *Proc. 2nd Int. Symp. Magnetic Bearings*, Tokyo, July 1990.
[6] C. R. Knospe, "Robustness of unbalance response controllers," in *Proc. 3rd Int. Symp. Magnetic Bearings*, Virginia, July 1992.
[7] T. Higuchi, T. Mizuno, and T. Tsukamoto, "Digital control for magnetic bearing with automatic balancing," in *Proc. 2nd Int. Symp. Magnetic Bearings*, Tokyo, July 1990.
[8] M. Fujita, K. Hatake, and F. Matsumura, "Loop shaping based robust control of a magnetic bearing," *IEEE Contr. Syst. Mag.*, vol. 13, no. 4, pp. 57–65, Aug. 1993.
[9] M. Fujita, K. Hatake, F. Matsumura, and K. Uchida, "Experiments on the loop shaping based H_∞ control of a magnetic bearing," in *Proc. 1993 American Control Conf.*, San Francisco, CA, pp. 8–12.
[10] D. McFarlane and K. Glover, "Robust controller design using normalized coprime factor plant descriptions," in *Lecture Notes in Control and Information Sciences*, vol. 138. Berlin: Springer-Verlag, 1990.
[11] T. Sugie, M. Fujita, and S. Hara, "Multiobjective controller design with the guaranteed H_∞ control performance," in *Proc. 12th IFAC World Congr.*, vol. 4, pp. 43–46, 1993.
[12] T. Sugie and S. Hara, "H_∞-suboptimal control problem with boundary constraints," *Syst. Contr. Lett.*, vol. 13, pp. 93–99, 1989.
[13] P. Apkarian, P. Gahinet, and G. Becker, "Self-scheduled H_∞ control of linear parameter-varying systems," in *Proc. American Control Conf.*, 1994, pp. 856–860.
[14] R. A. Hide and K. Glover, "The application of scheduled H_∞ controllers to a VSTOL aircraft," *IEEE Trans. Automat. Contr.*, vol. 38, no. 7, pp. 1021–1039, 1993.
[15] A. Packard, "Gain scheduling via linear fractional transformations," *Syst. Contr. Lett.*, vol. 22, no. 2, pp. 79–92, 1994.
[16] R. A. Nichols, R. T. Reichert, and W. J. Rugh, "Gain scheduling for H_∞ controllers: A flight control example," *IEEE Trans. Contr. Syst. Technol.*, vol. 1, no. 2, pp. 69–79, 1993.
[17] F. Matsumura, H. Kobayashi, and Y. Akiyama, "Fundamental equation of horizontal shaft magnetic bearing and its control system design," *Trans. IEE Japan*, vol. 101-C, no. 6, pp. 137–144, 1981 (in Japanese).
[18] F. Matsumura, M. Fujita, and K. Hatake, "Output regulation in magnetic bearing systems by a dynamic output feedback controller," *Trans. IEE Japan*, vol. 112-C, no. 10, pp. 977–983, 1992 (in Japanese).
[19] C. Checkoway, K. Kirk, D. Sullivan, and M. Townsend, *SIMULINK User's Guide*. Natick, MA: Math Works, 1992.

Fumio Matsumura (M'84) was born in Toyama, Japan, on July 27, 1935. He received the B.E. degree in electrical engineering from Kanazawa University, Japan, in 1958, and the D.E. degree from the University of Tokyo, Japan, in 1977.

Since 1958, he has been with Kanazawa University. He is currently a Professor in the Department of Electrical and Computer Engineering. His research interests are in control type magnetic suspension systems, magnetic bearings, and linear dc motors for industrial use.

Dr. Matsumura served as General Chair for the Fifth International Symposium on Magnetic Bearings in 1996.

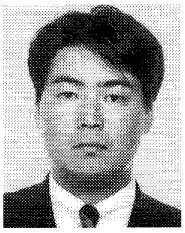

Toru Namerikawa (M'94) was born in Japan in 1968. He received the B.E. and M.E. degrees in electrical and computer engineering from Kanazawa University, Japan, in 1991 and 1993, respectively.

Since 1994, he has been with Kanazawa University. He is currently a Research Associate in the Department of Electrical and Computer Engineering. His research interests are in robust control applications and robotics and mechatronics.

Kazuhiko Hagiwara was born in Japan in 1971. He received B.E. and M.E. degrees in electrical and computer engineering from Kanazawa University, Japan, in 1994 and 1996, respectively.

He is with Fuji Electric Company, Limited. His research interests are in robust control of magnetic bearings.

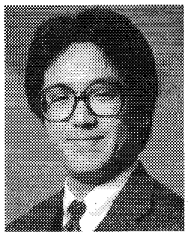

Masayuki Fujita (M'88) received the B.E., M.E., and Dr. of Engineering degrees in electrical engineering from Waseda University, Tokyo, in 1982, 1984, and 1987, respectively.

From 1985 until March 1992, he was with the Department of Electrical and Computer Engineering, Kanazawa University, Japan. In April 1992, he joined the Japan Advanced Institute of Science and Technology (JAIST), where he is presently an Associate Professor in the School of Information Science. From 1994 to 1995, he held a visiting position in the Deparment of Automatic Control Engineering, Technical University of Munich, Germany. His research interests include robust control and its applications to robotics and mechatronics.